현수교케이블의 응력부식에 관한 신뢰성해석

Reliability Analysis for Stress Corrosion Cracking of Suspension Bridge Wires

조 태 준*   Nowak, A.S.**

Taejun Cho   Andrzej S. Nowak

ABSTRACT

This paper deals with stress corrosion cracking behavior of high strength steel exposed to marine environments. The objective is to determine the time to failure as a function of hydrogen concentration and tensile stress in the wires. A crack growth curve is modeled using finite element method (FEM) program. The coupled hydrogen diffusion-stress analyses of SCC were programmed separately. The first part is calculating stress and stress intensity [1]factor of a cylindrical shell, prestressing tendon or suspension bridge wires, from the initiation of cracks to rupture. Virtual crack extension method, contour integral method, and crack tip elements are used for the calculation of stresses in front of the crack tip. Comparisons of the result show a good agreement with the analytical equations and wire tests. The second part of the study deals with the programming of hydrogen diffusion, affected by hydrostatic stress, calculated at the location of boundary of plastic area around the crack tip. The results of paper can be used in the design and management of prestressed structures, cable stayed and suspension bridges. Time dependent correlated parallel reliabilities of a cable, composed of 36 wires, were evaluated by the consideration of the deterioration of stress corrosion cracking.

1.Introduction

The overall environmental effects on crack growth can be termed as Environmental Assisted Cracking (EAC). This term Stress-corrosion cracking (SCC), Strain-induced corrosion cracking (SICC), and low cycle corrosion-fatigue (LCF). Stress-corrosion cracking (SCC) may be defined as a cracking process that requires three simultaneous actions of a corrosive, sustained tensile stresses and certain material properties. If the strain rate is lower than 10-1s-1, the type of corrosion is defined as low cycle corrosion fatigue [N. Eliaz and et al., 2002]. By contrast, if the strain rate is zero, it is defined as SCC.

As apposed to SCC, by SICC, fluctuating stress might cause initial imperfections, which

---

*   정회원, University of Michigan 박사과정
** University of Michigan 교수

could be the initiation of SCC. But, in this paper, the work is focused on the identification of the corrosion crack propagations, with zero strain rates, which occurs under static external loads. Thus, Stress-corrosion cracking model of a suspension bridge cable wire, have been studied in deterministic and probabilistic methods.

2. Fracture Analysis

2.1 Comparison with previous research

Figure 2.1 shows a thumb-nail shape stress corrosion crack in cable wire, tested by R.M. Mayrbaurl and et al. (2001). In 19 wire tests, the cracks lead to sudden brittle failure when the stress intensity factor at the crack tip is equal to the critical stress intensity factor, the fracture toughness Kc of the material. The stress intensity factor (SIF) for combined axial and bending stress is obtained by adding the results from the two formulas, given by Forman(1994), shown at Figure 2.3. The stress intensity factors (SIF) were calculated using the tensile strength of each specimen, the estimated crack depth, and the bending stress of 524 MPa that results from pulling the wire straight.

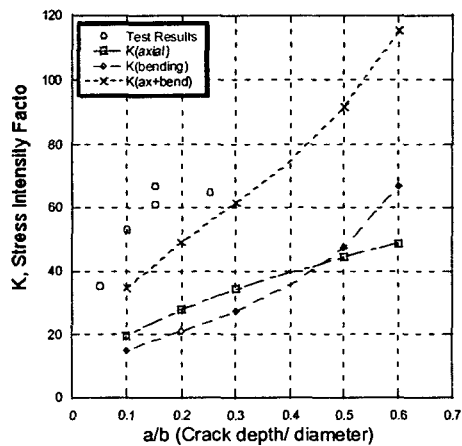Figure 2.1 Thumbnail crack by stress corrosion cracking of cable wire

Figure 2.2 Calculated SIF by axial, bending, combined external forces, and test results

As shown in Figure 2.2, the mean value of stress intensity factor, 62.2 MPa$\sqrt{m}$, is close in value to the test results, however, there is a discrepancy, if considering the crack depth/diameter ratio by the equation of Forman's(1994), as a maximum resisting loads, and the location of final crack propagations. The differences have been improved by the consideration of elastic-plastic material behavior, and contour integral methods.

At each crack propagation step, the stress intensity factors (SIF) were calculated by use of finite element program, ANSYS, with crack tip elements and plane 82 elements. Contour integral method was used for the SIF, and the values show excellent closeness with experimental results. The two calculations, which are based on elastic-plastic material model, in the Figure 2.3, show much improved results of SIF than Forman's equations, compared with the results of 19 wire

tests. The SIF of cross dotted line and triangle shape dotted line were calculated in elastic material model by the use of crack tip open displacements, and the SIF values can be calculated until the depth ratio (a/b)of 1.0.
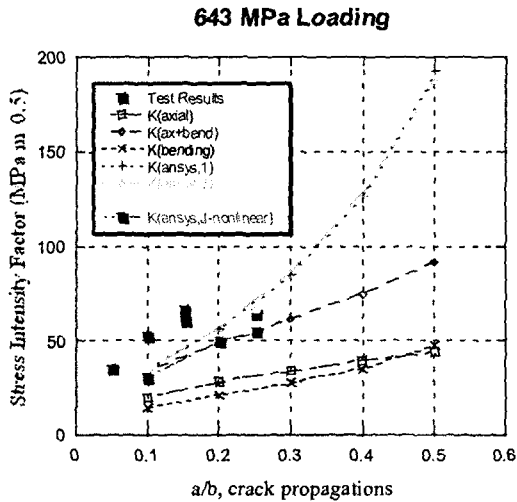
643 MPa Loading

Figure 2.3 Calculated SIF by elastic, and elastic-plastic material behavior, and test results

But, in the second calculation methods, SIF of round solid and rectangular dotted line were calculated in elastic-plastic material model, and the SIF values can be calculated until the depth ratio (a/b)of 0.22, at which the SIF show critical SIF, Kc. Thus, the expectations of service life time can be possible in this calculation technique. Detail descriptions of the model have been presented in the section 4.1.

2.2 Decoupling of diffusion-stress analysis

Decoupling method can give various merits, when applied to coupled problems, such as a diffusion-stress analysis. Using ready calculated stress intensity factors of each crack propagation steps, the time for calculations will be faster. In the author's judgments, if substructural analyses, dynamic analyses, and/or another coupled analyses are needed, only the decoupling and parallel programming can conduct the individual jobs successfully. It is necessary to emphasize that if analytical equivalent pressure (Equation 2.5) used, the crack growth results will be more exact, which was verified in ABAQUS example (version 6.3 example problems manual 6.1.2). Via Matlab programming, TSAHDA (Transient Stress Assisted Hydrogen Diffusion Analyses Program) has been developed for the evaluation of the hydrogen diffusion with crack growth (Section 4.3).

3.Stressassistedhydrogendiffusion

3.1 Diffusion Analysis

Diffusion is assumed to be driven by the gradient of a general chemical potential, which gives the behavior, considering a body with volume V and surface S, mass conservation requires the rate of change of total hydrogen inside V is equal to the flux through S:

$$\int_V \frac{dc}{dt}dV + \int_S n \cdot J dS = 0 \quad J = -D\nabla C + \frac{DCV_H}{RT}\nabla \sigma_h \tag{3.1}$$

where,

V is any volume whose surface is S,   n is the outward normal to S, and   is the

concentration flux leaving S. $\frac{\partial}{\partial t}$ is the partial derivative with respect to time, C is the hydrogen

concentration, n is the outward-pointing unit nominal vector and   is the flux of concentration of

the diffusing phase, D is diffusivity, VH is the partial molar volume of hydrogen, and $\nabla \sigma_h$ is the

gradient of hydrostatic stress. Substitution of equation 3.2and using the divergence theorem we

find,

$$\int_V \{\frac{\partial C}{\partial t} - \nabla \cdot (D\nabla C) + \nabla \cdot (\frac{DCV_H}{RT}\nabla \sigma)\}dV = 0 \tag{3.2}$$

3.2 Finite Element Diffusion Model

The governing equation of hydrogen diffusion in a plastically deforming body was introduced

in the previous section(Equation.3.3). Since the equation holds for an arbitrary volume V, the

integrand must vanish or

$$\frac{\partial C}{\partial t} - \nabla \cdot (D_L \nabla C_+) + \nabla \cdot (\frac{D_L C V_H}{RT}\nabla \sigma) = 0 \tag{3.3}$$

where, R is the universal gas constant, i.e. 8.3144 Jmol/K, T is the absolute temperature. The

governing equation can be written in matrix form:

$$[M][C'] + [K][C]-[F]=0 \tag{3.4}$$

where, $[M] = \int_V [N]^T D*[N]dV$, $[K1] = \int_V [B]^T D[B]dV$

$[K_2] = -\int_V [B]^T \frac{D_L \overline{V_H}}{RT}[B][\sigma_H][N]dV$, $[F] = \sum_{elements} \int_{S\phi} [N]^T \phi dS$

For convenience, the left-hand side of (Equation 3.8) is made symmetrically by putting the

term $[K_2][C]$ on the right-hand side:

$$[M][C']+[K_1][C]=[F]-[K_2][C] \tag{3.5}$$

A linear backward difference scheme was used for the discretization of the time variable. A

simple estimate of the matrices [M], [K], and [F] at $t+\Delta t$ can be made from the previous step,

results in

$$([M]_t + \Delta t[K_1])\{C\}^{t+\Delta t} = ([M]_t - \Delta t[K_2])\{C\}^t + \{F\}^t = 0 \tag{3.6}$$

The hydrostatic stress at the nodes is determined as follows:

$$p = -\frac{K(1+v)}{\sqrt{2\pi r}} - \frac{(1+v)\sigma}{3} \tag{3.7}$$

where, K is the stress intensity factor for a Mode I crack of length r and σ is the externally applied distributed load. With the use of the analytical values of equivalent pressure stress, the concentration solution by the FE program will show identical results with limited analytical concentration cases.

3.2 Crack Propagations

The mechanisms can be classed into two basic categories: anodic mechanisms and cathodic mechanisms. That is, during corrosion, both anodic and cathodic reactions must occur, and the phenomena that result in crack propagation may be associated with either type. The most obvious anodic mechanism is that of simple active dissolution and removal of material from the crack tip. The most obvious cathodic mechanism is hydrogen evolution, absorption, diffusion and embrittlement. However, a specific mechanism must be able to explain the actual crack-propagation rates, the fracto graphic evidence, and the mechanism of formation or nucleation of crack.[Barsom, John M.(1999)]

The critical concentration of hydrogen for crack propagations may be obtained from Sievert's law, Van Leeuwen's data (1974), and A. Krom's study (1998).

$$C = k\sqrt{p\exp\{(\frac{z_1}{T} + z_2)p\}}$$

(3.8)

where, k is solubility, z1 and z2 of 1.51e-6 K/Pa, and -1.04e-11 1/Pa.

Using the calculated pressure from previous volume-pressure relations, the critical concentrations of hydrogen at each step are decided.

4. Analyzed Model

4.1 Deterministic Model
4.1.1 Fracture model

Both elastic and elastic-plastic model have been tested in this calculations. In Figure 4.1, the text box shows two SIFs calculated form CTOD and Contour Integral methods.

4.1.2 Diffusion model

Figure 4.3 shows the cross section, at saddle area and boundary conditions, used for the calculations of hydrogen diffusion model. 2822. 4node, elements and 2940 nodes were used for the calculations of 17 to 44 crack propagation steps.

Since symmetric conditions used in this section, along the symmetric line, there be no hydrogen flux, and the initially charged hydrogen is assumed as initial condition value of c0.

4.2 Probabilistic Model
4.2.1 Ultimate limit states

For the System Reliability of a cable wire, under an environmental attack, the following ultimate limit state is selected: g (i,a,t)=ac-a(t)

(4.1)

where, i is ithwire in a cable, which will be used for the calculations of parallel system

reliability, a(t) is crack length of cable wire, varying with the age of cables, and ac is critical crack length. With the crack growth, increasing the ratio of crack depth/diameter, a/b, the tensile
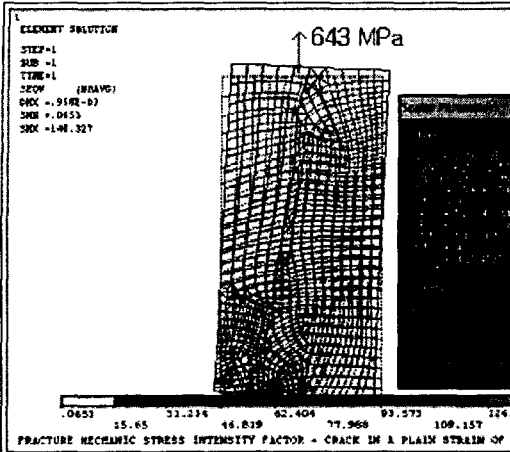

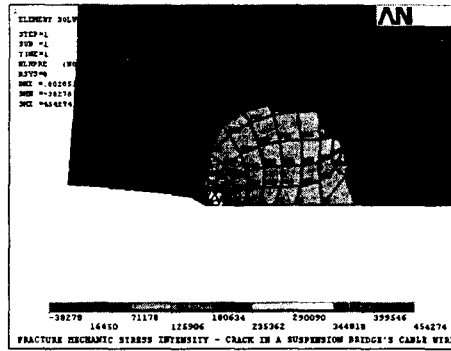Figure4.1 Principle stresses and stress intensity factors (SIF) with crack growth

Figure 4.2 Equivalent pressure around crack tip area, by external pressures with crack growth, crack depth/diameter=0.21

strength of the cable wire is decreased. Using the experimental data (Mayrbaurl et al.(2001)), mean value and variations of critical crack depth can be acquired, as Mean(ac) = 0.385 mm, V(ac) = 0.33.

Table 4.1 Parameters used in the calculations

Thermodynamic data	Mechanical parameters	Geometrical parameters
VH(mm3/mol)=2000 R(J/molK)=8.31422 T= 293(°K) D=4.58604E-10 m2/sec Co=3.1667e-6 mol/mm3	KIc= 62.2 MPa $\sqrt{m}$	Diameter=7mm H= 3.5 mm (with symmetric conditions) Δt=0.01 s
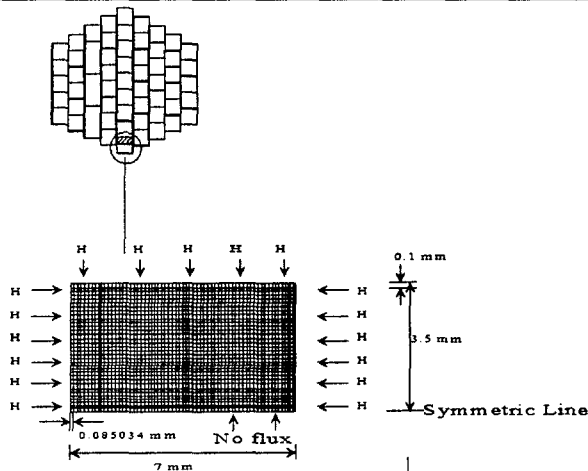
Figure 4.3 Used section of a cable wire, at saddle area and boundary conditions

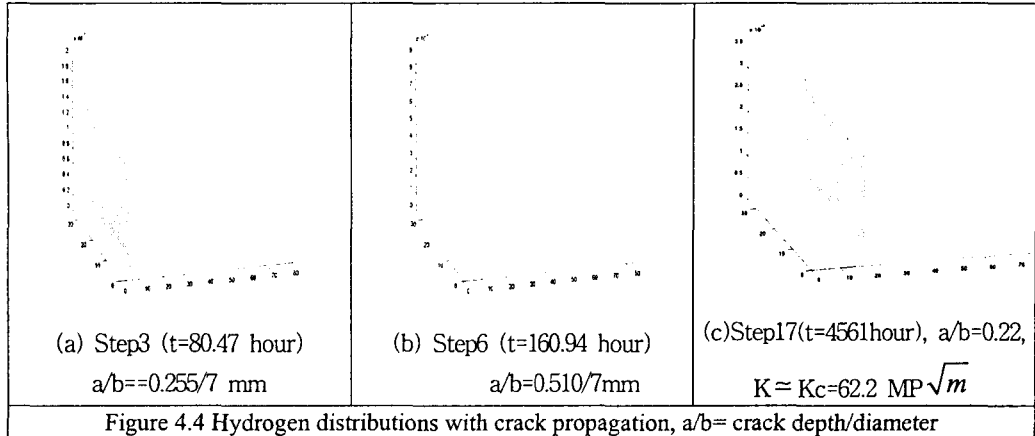| (a) Step3 (t=80.47 hour) a/b==0.255/7 mm	(b) Step6 (t=160.94 hour) a/b=0.510/7mm	(c)Step17(t=4561hour), a/b=0.22, $K \simeq Kc=62.2$ MP$\sqrt{m}$

Figure 4.4 Hydrogen distributions with crack propagation, a/b= crack depth/diameter

Considering the variation of diffusivities, the time-dependent safety of a cable wire can be evaluated, by the use of Equation 4.2,[A.S. Nowak (1999)]:

$$\beta(t) = \frac{a_{c)n}\lambda_{a_c}(1-kV_{a_c})[1-\ln(1-kV_{a_c})]-\overline{a(t)}}{\sqrt{[a_{c)n}V_{a_c}\lambda_{a_c}(1-kV_{a_c})]^2+\sigma^2_{a(t)}}} \qquad (4.2)$$

where, $a_{c)n}$ is nominal critical crack depth, λ_{a_c} is bias factor of critical crack depth, k =2, V_{a_c} is coefficient of variation of critical crack depth, $\overline{a(t)}$ is mean value of the time-dependent propagated crack depth, calculated from diffusion program TSAHDA (section 3.2), and $\sigma^2_{a(t)}$ is variation of the time-dependent propagated crack depth

4.3 SCC dependent System Reliability

Using the reliability of individual wires by Equation 4.2, the parallel system reliability can be acquired as follows from the parallel probabilities of failure:

$$\prod_{i=1}^{n} P_{fi}(t) \leq P_f(t) \leq \min(P_{fi}(t)) \qquad (4.3)$$

Considering 128, as the number of cable wires, time-dependent system reliability of a cable is evaluated (Figure 4.6). Due to huge number of wires, the reliability of a cable show almost zero of probability of failure as a lower bound value (Figure4.8). Upper bound of the probability of system failure is decided by the minimum value of a failure of a wire. Although the calculation is assumed as uncorrelated random variables, the correlated cases also will be in the range of equation 4.3. Considering the parallel system's probability of failure between 128 and 64 wires, because there be a little difference in the probability of failure, the author would suggest changing of current cable to two cables, composed of 64 wires. By the changing, the upper bound of probability of failure will be reduced, almost without changing of lower bound value. The system reliability of whole cables will be increased, and the cost for replacing of a cable will be reduced as well. However, still we need to consider the correlated cases for narrowing the evaluations of probability of

failures.

In addition to that, with the crack growing, due to the decreasing of strength of a cable and the variations of resistance by a wire, the structural system analyses also need to combine with the calculations given in this paper.
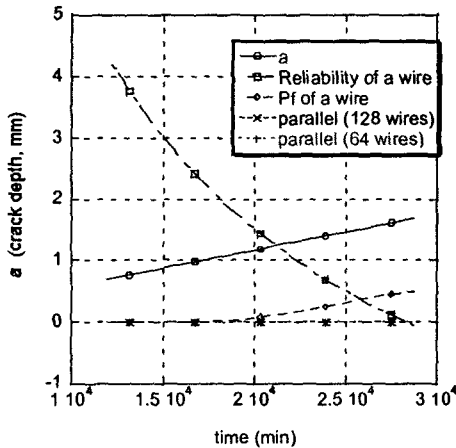

Figure 4.6 Time dependent Reliabilities and The Probabilities of Failures with crack growth, a, for individual cable wire and for a cable (128 wire and 64 wire cases)

4. Conclusions and Further Study

Considering the parallel system's probability of failure between 128 and 64 wires, because there be a little difference in the probability of failure, the author would suggest changing of current cable to two cables, composed of 64 wires. By the changing, the upper bound of probability of failure will be reduced, almost without changing of lower bound value. The system reliability of whole cables will be increased, and the cost for replacing of a cable will be reduced as well. However, still we need to consider the correlated cases for narrowing the evaluations of probability of failures.

From this pilot studying of hydrogen diffusion with crack propagations, approximate solutions have been evaluated. The circular section models, residual stress effects, amplitude loadings, correlated random variables, and structural system analyses need to be studied more.

REFERENCES

Andrzej S. Nowak, (1999), "Calibration of LRFD Bridge Design Code", Report368, TRB, NCHRP, National Academy Press, W.C., 1999

Forman R.G. and Shivakuma V. (1986), Fracture Mechanics, Vol17, ASTM STP 905, pp. 59-74

R.M. Mayrbaurl, S.Camo, (2001), Cracking and Fracture of Suspension Bridge Wire, Journal of Bridge Engineering, Nov.2001, pp 645-650